

Title : Streamlining and large ancestral genomes in Archaea inferred with a phylogenetic birth-and-death model

Authors : Miklós Csűrös¹ and István Miklós²

Authors' affiliations: ¹ Department of Computer Science and Operations Research, University of Montréal, Canada. ² Rényi Institute of Mathematics, Hungarian Academy of Sciences, Budapest, Hungary.

Corresponding author: Miklós Csűrös. Département d'informatique et de recherche opérationnelle, Université de Montréal, C.P. 6128, succursale Centre-Ville, Montréal, QC, H3C 3J7, Canada. Tel: +1 514 343-6111 extension 1655. Fax: +1 514 343-6111. E-mail: csuros@iro.umontreal.ca.

Abstract

1
2 Homologous genes originate from a common ancestor through vertical
3 inheritance, duplication or horizontal gene transfer. Entire homolog fam-
4 ilies spawned by a single ancestral gene can be identified across multiple
5 genomes based on protein sequence similarity. The sequences, however, do
6 not always reveal conclusively the history of large families. In order to study
7 the evolution of complete gene repertoires, we propose here a mathematical
8 framework that does not rely on resolved gene family histories. We show
9 that so-called phylogenetic profiles, formed by family sizes across multiple
10 genomes, are sufficient to infer principal evolutionary trends. The main nov-
11 elty in our approach is an efficient algorithm to compute the likelihood of
12 a phylogenetic profile in a model of birth-and-death processes acting on a
13 phylogeny.

14 We examine known gene families in 28 archaeal genomes using a proba-
15 bilistic model that involves lineage- and family-specific components of gene
16 acquisition, duplication, and loss. The model enables us to consider all pos-
17 sible histories when inferring statistics about archaeal evolution. According
18 to our reconstruction, most lineages are characterized by a net *loss* of gene
19 families. Major increases in gene repertoire have occurred only a few times.
20 Our reconstruction underlines the importance of persistent streamlining pro-
21 cesses in shaping genome composition in Archaea. It also suggests that early
22 archaeal genomes were as complex as typical modern ones, and even show
23 signs, in the case of the methanogenic ancestor, of an extremely large gene
24 repertoire.

25 **Introduction**

26 The evolution of homologous gene families, i.e., genes of common ancestry, is
27 enmeshed within species histories in a complex manner (Koonin, 2005). Con-
28 comitantly with the diversification of organismal lineages, gene families expand
29 by duplications, individual genes get eliminated, and new genes arrive by lateral
30 transfer. It is now clear that *de novo* gene formation and vertical processes (Snel
31 *et al.*, 2002; Henikoff *et al.*, 1997), such as duplication and loss, act in concert with
32 horizontal gene transfer (Boucher *et al.*, 2003; Gogarten and Townsend, 2005).

33 Gene families are identified in current practice by pairwise sequence compar-
34 isons, coupled with the clustering of postulated homolog pairs (Tatusov *et al.*,
35 1997; Alexeyenko *et al.*, 2006) The phylogenetic profile of a gene family com-
36 prises the family size across a set of organisms, i.e., the number of homologs within
37 the same family in each genome. Such profiles are extremely informative even
38 without taking the gene sequences into account: profile data sets have been used
39 to construct organismal phylogenies (Fitz-Gibbon and House, 1999; Snel *et al.*,
40 1999; Tekaiia *et al.*, 1999) and to infer ancestral gene content (Mirkin *et al.*, 2003;
41 Iwasaki and Takagi, 2007); similar and complementary profiles hint at functional
42 associations (Tatusov *et al.*, 1997; Pellegrini *et al.*, 1999). Considering various
43 evolutionary processes in a mathematical model of gene family evolution is chal-
44 lenging. One main element that distinguishes the present study from past work
45 is the elaboration of a likelihood framework for phylogenetic profiles that simul-
46 taneously accounts for gene duplication, loss, and acquisition. In particular, we
47 describe an algorithm for the exact computation of the likelihood in a phylogenetic
48 gain-loss-duplication model.

49 The present study uses a gain-loss-duplication model to address gene content
50 evolution in Archaea. Relying on a complete set of known homolog families in 28
51 sequenced genomes, we inferred lineage- and family-specific statistics. In a pre-
52 cursory step, we constructed a plausible phylogeny using 88 universally conserved
53 proteins, which we believe is a noteworthy result on its own, as the phylogeny
54 resolves some problematic euryarchaeal branching orders (involving Thermoplas-
55 matales, Methanopyrus and Methanobacteriales) confidently. Gene loss emerges
56 in our analysis as the dominant force that has shaped archaeal genomes through-
57 out their history. Apparently, genome streamlining has been an ongoing process
58 in all lineages with a fairly constant intensity, apart from dramatic genome com-
59 pactions in endosymbiotic Archaea. Our reconstruction suggests that early Ar-
60 chaea had a comparable genomic complexity to today's organisms. In particular,
61 the euryarchaeal ancestor of two classes of methanogens had a very large genome,
62 resulting from one of the rare upsurges in gene content, similarly to some modern
63 lineages of Methanosarcina and Halobacteria.

64 **Methods**

65 **Phylogenetic profiles in Archaea**

66 Phylogenetic profiles, sequences, and functional annotations were downloaded from
67 the arCOG database of orthologous gene clusters in Archaea (Makarova *et al.*,
68 2007) at <ftp://ftp.ncbi.nih.gov/pub/wolf/COGs/arCOG>. The pro-
69 files were amended with data on lineage-specific singletons and inparalog families
70 that have no archaeal homologs outside of one genome (Yuri Wolf, personal com-
71 munication), which was produced in the process of compiling the arCOG database.

72 The following organisms are included in the study: *Archaeoglobus fulgidus*
73 (Arcfu), *Haloarcula marismortui* ATCC 43049 (Halma), *Halobacterium* sp. strain
74 NRC-1 (Halsp), *Methanosarcina acetivorans* (Metac), *Methanococcoides burtonii*
75 DSM 6242 (Metbu), *Methanoculleus marisnigri* JR1 (Metcu), *Methanospirillum*
76 *hungatei* JF-1 (Methu), *Methanocaldococcus jannaschii* (Metja), *Methanopyrus*
77 *kandleri* (Metka), *Methanosarcina mazei* (Metma), *Methanococcus maripaludis*
78 S2 (Metmp), *Methanosphaera stadtmanae* (Metst), *Methanothermobacter thermoau-*
79 *totrophicus* (Metth), *Nanoarchaeum equitans* (Naneq), *Picrophilus torridus* DSM
80 9790 (Picto), *Pyrococcus abyssi* (Pyrab), *Pyrococcus furiosus* (Pyrfu), *Thermo-*
81 *plasma acidophilum* (Theac), *Thermococcus kodakaraensis* KOD1 (Theko), *Ther-*
82 *moplasma volcanium* (Thevo), *Aeropyrum pernix* (Aerpe), *Caldivirga maquilin-*
83 *gensis* IC-167 (Calma), *Cenarchaeum symbiosum* (Censy), *Hyperthermus butylicus*
84 (Hypbu), *Pyrobaculum aerophilum* (Pyræ), *Sulfolobus solfataricus* (Sulso); *Sul-*
85 *folobus acidocaldarius* DSM 639 (Sulac), *Thermofilum pendens* Hrk 5 (Thepe)
86 with the last eight classified as crenarchaeota. The abbreviations are those used
87 by (Makarova *et al.*, 2007) and the arCOG database.

88 **Reconstruction of archaeal phylogeny**

89 The phylogeny was constructed using concatenated multiple alignments of se-
90 lected orthologous protein sequences. The sequences were chosen from the arCOG
91 database based on phylogenetic profiles: we selected all arCOG groups where ev-
92 ery studied genome contained exactly one homolog. There are 88 such groups
93 (see Supplemental Material for sequences), and 46 of those correspond to ribo-
94 somal proteins. Alignments were done using the program Muscle (Edgar, 2004).
95 Phylogenies were built by likelihood maximization using PhyML (Guindon and
96 Gascuel, 2003), with the Jones-Taylor-Thornton substitution model and eight dis-
97 crete Gamma categories and invariant sites. The expected number of substitutions
98 per amino acid site was computed on each edge for the ribosomal proteins in the
99 JTT+I+ Γ 8 model by PhyML. Bootstrap support values for the branches were com-
100 puted by PhyML, using 500 replicates.

101 **Inference of gene content evolution**

102 We maximized the likelihood (see below for the likelihood computation) of the
103 data set using a gain-loss-duplication model with a Poisson distribution at the root
104 and four discrete Gamma categories capturing rate variation across families, for
105 edge length t_f and duplication λ_f each. For a given set of model parameters (three
106 parameters — $\hat{t}_e \hat{\kappa}_e$, $\hat{t}_e \hat{\mu}_e$, $\hat{t}_e \hat{\lambda}_e$ — per edge, one for the root's Poisson param-
107 eter Γ , and two Gamma shape parameters for rate variation), the likelihood of
108 each family was computed using (1) with the described methods of manipulating
109 rate variation and correcting for absent profiles. The data set's likelihood (i.e.,
110 the product of family likelihoods) was then maximized numerically as a function

111 of the model parameters, using custom-made software implementing the Broyden-
 112 Fletcher-Goldfarb-Shanno conjugate gradient method and Brent’s one-dimensional
 113 optimization method (Press *et al.*, 1997). Family sizes and lineage-specific events
 114 (gains, losses, expansions, contractions) were computed using posterior probabilities
 115 in the optimized gain-loss-duplication model.

116 **Phylogenetic birth-and-death model**

117 A *phylogenetic birth-and-death model* formalizes the evolution of an organism-
 118 specific census variable along a rooted phylogeny T . We consider only binary
 119 phylogenies here; the full set of methods applicable to multi-furcating phylogenies
 120 is described in the Supporting Information. The model specifies edge lengths, as
 121 well as birth-and-death processes (Ross, 1996; Kendall, 1949) acting on the edges.
 122 Populations of identical individuals evolve along the tree from the root towards
 123 the leaves by Galton-Watson processes. At non-leaf nodes of the tree, populations
 124 are instantaneously copied to evolve independently along the adjoining descen-
 125 dant edges. Let the random variable $\xi(x) \in \{0, 1, 2, \dots\}$ denote the population
 126 count at every node $x \in \mathcal{V}(T)$. Every edge xy is characterized by a loss rate μ_{xy} ,
 127 a duplication rate λ_{xy} and a gain rate κ_{xy} . If $(X(t): t \geq 0)$ is a linear birth-
 128 and-death process (Kendall, 1949; Takács, 1962) with these rate parameters, then
 129 $\mathbb{P}\{\xi(y) = m \mid \xi(x) = n\} = \mathbb{P}\{X(t_{xy}) = m \mid X(0) = n\}$, where $t_{xy} > 0$ is
 130 the edge length, which defines the time interval during which the birth-and-death
 131 process runs. The joint distribution of $(\xi(x): x \in \mathcal{V}(T))$ is determined by the phy-
 132 logeny, the edge lengths and rates, along with the distribution at the root ρ , denoted
 133 as $\gamma(n) = \mathbb{P}\{\xi(\rho) = n\}$.

134 It is assumed that one can observe the population counts at the terminal nodes

135 (i.e., leaves), but not at the inner nodes of the phylogeny. Since individuals are
 136 considered identical, we are also ignorant of the ancestral relationships between in-
 137 dividuals within and across populations. The population counts at the leaves form
 138 a *phylogenetic profile*, which is formally a function $\Phi: \mathcal{L}(T) \mapsto \{0, 1, 2, \dots\}$,
 139 where $\mathcal{L}(T) \subset \mathcal{V}(T)$ denote the set of leaf nodes. Our central problem is to com-
 140 pute the likelihood of a profile, i.e., the probability of the observed counts for fixed
 141 model parameters. Define the notation $\Phi(\mathcal{L}') = (\Phi(x): x \in \mathcal{L}')$ for the partial
 142 profile within a subset $\mathcal{L}' \subseteq \mathcal{L}(T)$. Similarly, let $\xi(\mathcal{L}') = (\xi(x): x \in \mathcal{L}')$ denote
 143 the vector-valued random variable composed of individual population counts. The
 144 *likelihood* of Φ is the probability $L = \mathbb{P}\{\xi(\mathcal{L}(T)) = \Phi\}$. Let T_x denote the sub-
 145 tree of T rooted at node x . Define the *survival count range* M_x for every node x as
 146 $M_x = \sum_{y \in \mathcal{L}(T_x)} \Phi(y)$. Clearly, the ranges can be calculated easily in a postorder
 147 traversal.

148 For our discussion, we borrow standard terminology applied to homologous
 149 genes (Sonnhammer and Koonin, 2002). For every edge xy , the population of
 150 node y can be split by ancestry at node x : *inparalog* groups are formed by the
 151 progenies of each individual at x and a *xenolog* group is formed by the individuals
 152 whose ancestor immigrated into the population. When $\xi(x) = n$ on the edge xy ,
 153 then $\xi(y) = \eta + \sum_{i=1}^n \zeta_i$, where η is the xenolog group size, and ζ_i are the indepen-
 154 dent and identically distributed inparalog group sizes. The distribution of xenolog
 155 and inparalog group sizes is the well-characterized transient distribution of the ap-
 156 propriate linear birth-and-death processes (Karlin and McGregor, 1958; Kendall,
 157 1949; Takács, 1962); see Supplemental Material. Namely, each ζ_i has a shifted
 158 geometric distribution, and for $\kappa > 0$, η has a negative binomial or Poisson distri-
 159 bution. The distributions' parameters are known functions of the edge length t_{xy}

160 and rates $\kappa_{xy}, \lambda_{xy}, \mu_{xy}$.

161 **Surviving lineages**

162 A key factor in inferring the likelihood formulas is the probability that a given in-
163 dividual at a tree node x has no descendants at the leaves within the subtree rooted
164 at x . The corresponding *extinction probability* is denoted by D_x , which can be
165 computed in a postorder traversal (Csűrös and Miklós, 2006). An individual at
166 node x is referred to as *surviving* if it has at least one progeny at the leaves de-
167 scending from x . Let $\Xi(x)$ denote the number of surviving individuals at each
168 node x . The number of surviving xenologs and inparalogs follow the same class of
169 distributions as the total number of xenologs and inparalogs (see Supplemental Ma-
170 terial). Consequently, if $\xi(x) = n$ on edge xy , then $\Xi(y) = \eta + \sum_{i=1}^n \zeta_i$, where η
171 is the surviving xenolog count with a Poisson or negative binomial distribution, and
172 ζ_i are surviving paralog counts, with negative binomial distributions. The distri-
173 butions' parameters can be computed explicitly using the process parameters and
174 the extinction probabilities. In the formulas to follow, we use the probabilities
175 $w_y^*[m|n] = \mathbb{P}\{\eta + \sum_{i=1}^n \zeta_i = m; \forall \zeta_i > 0\}$, which can be computed by dynamic
176 programming for all $n, m \leq M_y$ in $O(M_y^2)$ time (see Supplemental Material).

177 **Computing the likelihood**

178 We compute the likelihood using *conditional survival likelihoods* defined as the
179 probability of observing the partial profile within T_x given the number of surviving
180 individuals $\Xi(x)$: $L_x[n] = \mathbb{P}\left\{\xi(\mathcal{L}(T_x)) = \Phi(\mathcal{L}(T_x)) \mid \Xi(x) = n\right\}$. For $m >$
181 M_x , $L_x[m] = 0$. For values $m = 0, 1, \dots, M_x$, the conditional survival likelihoods
182 can be computed recursively as shown below.

If node x is a leaf, then

$$L_x[n] = \begin{cases} 0 & \text{if } n \neq \Phi(x); \\ 1 & \text{if } n = \Phi(x). \end{cases}$$

If x is an inner node with children x_1, x_2 , then $L_x[n]$ can be expressed using $L_{x_i}[\cdot]$ and auxiliary values $B_{i;\cdot}$, for $i = 1, 2$ in the following manner. Auxiliary values $B_{i;t,s}$ are defined for $i = 1, 2$ and $s = 0, \dots, M_{x_i}$ as follows.

$$B_{i;0,s} = \sum_{m=0}^{M_{x_i}} w_{x_i}^*[m|s] L_{x_i}[m] \quad \{0 \leq s \leq M_{x_i}\}$$

$$B_{2;t,M_{x_2}} = G_{x_2}(0) B_{2;t-1,M_{x_2}}$$

$$B_{2;t,s} = B_{2;t-1,s+1} + G_{x_2}(0) B_{2;t-1,s} \quad \{0 \leq s < M_{x_2}\}$$

184 where $G_{x_i}(k) = \mathbb{P}\{\zeta = k\}$ for a surviving inparalog group at x_i . In the above
185 equations, $0 < t \leq M_{x_1}$. For all $n = 0, \dots, M_x$

$$L_x[n] = (1 - D_x)^{-n} \sum_{\substack{0 \leq t \leq M_{x_1} \\ 0 \leq s \leq M_{x_2} \\ t+s=n}} \binom{n}{s} (D_{x_1})^s B_{1;0,t} B_{2;t,s}.$$

186 The complete likelihood is computed as

$$L = \sum_{m=0}^{M_\rho} L_\rho[m] \mathbb{P}\{\Xi(\rho) = m\}.$$

187 For some parametric distributions γ , there is a closed formula for $\mathbb{P}\{\Xi(\rho) = m\}$. In
188 particular, if γ is the stationary distribution for a gain-loss-duplication or a gain-loss

189 models, then $\Xi(\rho)$ has a negative binomial or Poisson distribution, respectively.

190 The likelihood for a Poisson distribution at the root is

$$L = \sum_{m=0}^{M_\rho} L_\rho[m] \exp\left(-\Gamma(1 - D_\rho)\right) \frac{(\Gamma(1 - D_\rho))^m}{m!} \quad (1)$$

191 where Γ is the mean family size at the root.

192 The likelihood formula (1) is corrected in order to account for the fact that the
193 data set does not contain all-absent profiles with $\Phi(x) = 0$ for all leaves x , in a
194 manner analogous to (Felsenstein, 1992).

195 Family-specific rate variation is considered by computing the likelihood val-
196 ues for each discrete rate category c characterized by factors $(t_c, \kappa_c, \mu_c, \lambda_c)$. The
197 factors in our analysis are either constant 1, or correspond to the expected values
198 within the four quartiles of a Gamma distribution with mean 1.

199 **Results and discussion**

200 **Computational analysis of phylogenetic profiles**

201 Birth-and-death processes are commonly used to model a population of identi-
202 cal individuals (Kendall, 1949; Karlin and McGregor, 1958) and waiting queues
203 (Takács, 1962). Their use in modeling gene family evolution is justified by the
204 fact that losses and duplications seem to occur independently between the mem-
205 bers of multi-gene families (Nei and Rooney, 2005). The most general process we
206 consider is a gain-loss-duplication process which is characterized by the rates of
207 gain κ , loss μ and duplication λ : a population of size n grows by a rate of $(\lambda n + \kappa)$
208 and decreases by a rate of μn . In our context, the population comprises homologs
209 of a given family in the genome. Gene acquisition occurs with a rate of κ , combin-
210 ing various means such as innovation and lateral transfer. We model gene family
211 evolution in a phylogenetic setting by associating gain-loss-duplication processes
212 with the branches of a phylogenetic tree. The corresponding phylogenetic birth-
213 and-death model defines a probabilistic framework for the evolution of gene family
214 size. The observed family sizes at the terminal nodes form a phylogenetic profile.
215 In principle, a phylogenetic birth-and-death model suits likelihood-based inference
216 since it is a probabilistic graphical model (Jordan, 2004) with a tree structure. The
217 mathematical difficulties stem from the fact that the state space of the processes
218 (i.e., family size) is infinitely large. Consequently, routine computational tech-
219 niques used to analyze molecular sequence evolution (Felsenstein, 1981) are not
220 applicable. Previously proposed likelihood methods (Hahn *et al.*, 2005; Spencer
221 *et al.*, 2006; Iwasaki and Takagi, 2007) have sidestepped the infinity problem by

222 using approximative calculations with bounds on maximal family size.

223 We have introduced (Csűrös and Miklós, 2006) a procedure for computing
224 the likelihood in a restricted gain-loss-duplication model (assuming $0 < \kappa$ and
225 $0 < \lambda < \mu$), without imposing artificial size bounds. The weakness of that pro-
226 cedure is potential numerical instability, due to the use of alternating sums in the
227 formulas. We found practical cases (such as the archaeal gene content study we
228 report below), where the numerical instability led to serious errors. The novel pro-
229 cedure presented here is numerically stable, as well as computationally efficient. It
230 applies to arbitrary gain-loss-duplication models, including degenerate cases such
231 as the one of (Hahn *et al.*, 2005) with $\lambda = \mu$ and $\kappa = 0$. The algorithm takes
232 $O(M^2n)$ time to complete for a phylogenetic profile over n species and M total
233 number of genes (see Supplemental Material).

234 **Gene content evolution in Archaea**

235 Archaea constitute one of the three main domains of cellular life, and are notable
236 for a spectacular diversity of adaptive strategies to extreme environments (Garrett
237 and Klenk, 2006). We examined gene content evolution in Archaea. For the pur-
238 poses of the study we have selected 28 completely sequenced genomes covering all
239 major physiological and metabolic groups recognized in cultured Archaea: ther-
240 mophiles, halophiles, acidophiles, nitrifiers and methanogens (Valentine, 2007).
241 Homolog gene families were extracted from the arCOG (archaeal clusters of or-
242 thologous groups) database (Makarova *et al.*, 2007), and combined with groupings
243 of genes that have no archaeal homologs outside of single genomes. The complete
244 data set consists of 14216 families, of which 7461 are among the arCOGs.

245 **Phylogenetic relationships**

246 Archaeal phylogenetic relationships have been resolved to an increasing degree
247 of confidence (Forterre *et al.*, 2006) with the aid of accumulating sequence data.
248 Figure 1 shows our consensual phylogeny based on maximum likelihood trees for
249 concatenated alignments of 46 ribosomal proteins (r-proteins) and 88 unique con-
250 served proteins (uc-proteins), which are precisely those that have exactly one ho-
251 molog in each sampled genome. Congruent phylogenies were proposed before
252 (Forterre *et al.*, 2006; Gribaldo and Brochier-Armanet, 2006), based on complete
253 phylogenomics evidence. In our study, r-proteins and uc-proteins show solid sup-
254 port for most recognized phylogenetic relationships, but provide contradictory sig-
255 nals for the placement of some euryarchaeal groups. Notably, both sequence data
256 sets support the basal position of *N. equitans*, which was originally thought to be a
257 specimen of a separate group from Euryarchaeota and Crenarchaeota (Waters *et al.*,
258 2003), but is more likely an early-branching euryarchaeal organism (Makarova and
259 Koonin, 2005; Forterre *et al.*, 2006). The data also support the early branching po-
260 sition of non-thermophilic crenarchaea represented by *C. symbiosum*. In fact, non-
261 thermophilic crenarchaea may constitute a separate phylum from Euryarchaeota
262 and Crenarchaeota, tentatively named Thaumarchaeota (Brochier-Armanet *et al.*,
263 2008).

264 [Figure 1 about here.]

265 The observed uncertainties about euryarchaeal groups concern the placement
266 of Thermoplasmata, and so-called Class I methanogens (Baptiste *et al.*, 2005)
267 comprising Methanopyrales, Methanobacteriales and Methanococcales. Thermo-
268 plasmata were originally thought to be a an early-branching lineage of Euryarchaeota

269 (Forterre *et al.*, 2006), but analyses of r-proteins (Matte-Tailliez *et al.*, 2002) have
270 provided strong evidence for their late-branching position after Class I methanogens
271 as in Figure 1. R-proteins in our study support the late-branching of Thermo-
272 plasmatales (89% bootstrap value), but a maximum-likelihood tree built from uc-
273 proteins places Thermoplasmatales between Nanoarchaea and Thermococcales (66%
274 BV). It has been argued that this placement is due to long-branch attraction (Matte-
275 Tailliez *et al.*, 2002; Brochier *et al.*, 2004), a frequent systematic bias of sequence
276 evolution models (Rodríguez-Ezpeleta *et al.*, 2007). Indeed, after we removed
277 *N. equitans* and *C. symbiosum* from the uc-protein data set, the late-branching po-
278 sition of Thermoplasmatales regained solid support (100% BV).

279 The correct phylogenetic position of *M. kandleri* (Metka) is one of the re-
280 maining puzzles in archaeal evolution. The existence of close phylogenetic re-
281 lationships between Class I methanogens is fairly certain, but different protein
282 sets and taxonomic sampling give conflicting or weak indications (Slesarev *et al.*,
283 2002; Brochier *et al.*, 2004, 2005; Gao and Gupta, 2007) about the exact branch-
284 ing order among Methanopyrales, Methanobacteriales and Methanococcales. R-
285 proteins in our study give a weak support for the monophyly of Methanococcales
286 and Methanobacteriales at the exclusion of Methanopyrales (49% BV) and faintly
287 favor the paraphyly of Class I methanogens (37% BV for the immediate split of
288 Methanopyrales between Thermococcales and Methanobacteriales/Methanococcales;
289 see Supplemental Material). Uc-proteins, however, solidly point to the monophyly
290 of Class I methanogens (> 97% BV). Interestingly, the maximum-likelihood trees
291 built from uc-proteins do not resolve well the relationships between Halobacteri-
292 ales, Methanosarcinales and Methanomicrobiales (see Supplemental Material), but
293 there is little reason to doubt that r-proteins provide a genuine phylogenetic signal

294 about the monophyly of Class II methanogens (Baptiste *et al.*, 2005; Brochier-
295 Armanet *et al.*, 2008), uniting Methanosarcinales and Methanomicrobiales.

296 We conclude that based on protein sequences, Thermoplasmatales constitute
297 a late-branching euryarchaeal lineage, and their early-branching status is a long-
298 branch attraction artifact. Furthermore, the sequences provide evidence of the
299 monophyly of both Class I and Class II methanogens.

300 **Evolutionary rates: correlations between sequence and gene content** 301 **evolution**

302 We experimented with models of increasing complexity that combine lineage- and
303 gene-specific factors in the gain-loss-duplication processes. Specifically, we as-
304 sumed that the process for family f on branch e is characterized by the rates
305 $\kappa = \hat{\kappa}_e \kappa_f$, $\mu = \hat{\mu}_e \mu_f$, $\lambda = \hat{\lambda}_e \lambda_f$, and runs for a duration of $t = \hat{t}_e t_f$. Here,
306 $\hat{t}_e, \hat{\kappa}_e, \hat{\mu}_e, \hat{\lambda}_e$ are branch-specific process parameters, and $t_f, \kappa_f, \mu_f, \lambda_f$ are family-
307 specific rate variation coefficients. Starting with simple models with invariant
308 family-specific coefficients, we introduced rate variation in a model hierarchy with
309 increasing complexity. In more complex models, some coefficients were drawn
310 randomly from a discretized Gamma distribution (Yang, 1994). Different family-
311 specific coefficients do not have the same impact on the model fit. We found the
312 largest improvement when introducing variation in edge length (t_f), followed by
313 duplication-rate variation (λ_f). Further variation in loss and gain rates led to in-
314 significant improvements in the model fit, and were not assumed in the analysis.

315 [Figure 2 about here.]

316 In the absence of extraneous scaling, we set $\hat{t}_e = 1$ in order to examine the total
317 rates of gene content change on each edge e . We found a conspicuous correlation
318 across branches between the rate of sequence evolution (expected numbers of sub-
319 stitutions per site for ribosomal proteins) and the component rates of gene content
320 evolution: on this point, see Figure 2 for loss, and the Supplemental Material for
321 duplication and gain. More precisely, the correlation holds for the lineage-specific
322 components of loss, duplication and gain rates in a decreasing order of strength
323 (P -values of $1.1 \cdot 10^{-11}$, $8.2 \cdot 10^{-6}$, $1.6 \cdot 10^{-4}$, respectively, by Student's t -test for
324 Spearman rank-order correlation coefficient).

325 The apparent correlations between gene content and sequence evolution rates
326 imply that a steady balance has been maintained between drift and natural selec-
327 tion in almost all lineages. Loss and duplication rates, in particular, have similar
328 vagaries as amino acid substitution rates, and provide thus comparable molecu-
329 lar clocks. We measured each terminal node's depth by summing the rates along
330 branches from the root to the node in question. Excluding *N. equitans* and *C. sym-*
331 *biosum*, the coefficient of variation of the depth is 26% for protein sequences, 23%
332 for gene loss rates and 20% for duplication rates. Depths by gene gain rates span
333 about a four-fold range: for substitution, loss, and duplication, the span is close to
334 two-fold.

335 Genes have thus been eliminated in all archaeal lineages with a fairly universal
336 constancy, apart from occasional accelerations. In other words, genome degrada-
337 tion processes seem to persist at a fairly common intensity in every lineage (Mira
338 *et al.*, 2001). Conceivably, genome decay is counterbalanced by natural selection
339 that eliminates deleterious mutations. The root cause of dramatically increased
340 gene loss in obligate symbionts such as *N. equitans* (Makarova and Koonin, 2005)

341 may be reduced selection (Hershberg *et al.*, 2007; Koonin and Wolf, 2008). Princi-
342 ples of population genetics imply that changes in population size alone can explain
343 rate changes (Lynch, 2006): selection power is weaker in a smaller population,
344 which should manifest in accelerated evolution of sequences (Ohta, 1972) and gene
345 content.

346 We examined the differences between evolutionary rates in sibling terminal
347 taxa for signs of natural selection. Figure 2 shows that gene loss and amino
348 acid substitution rates differ in a concerted fashion for three pairs, that is, for
349 *M. stadtmanæ*-*M. thermoautotrophicus*, *Halobacterium* sp.-*H. marismortuimi*, and
350 *S. acidocaldarius*-*S. sulfolobus*. In seven other pairs, loss rates are essentially the
351 same, even if substitution rates may differ. The agreements between substitution
352 and gene loss rate changes attest to common selection forces and mutation pro-
353 cesses acting on different forms of genome decay, and are predicted by population-
354 genetic arguments (Lynch, 2006).

355 In the lineage leading to *M. stadtmanæ*, a human commensal (Fricke *et al.*,
356 2006), all rates are simultaneously larger when compared to its sibling lineage
357 *M. thermoautotrophicus*, which may be attributed to a smaller population size for
358 the former, which has a smaller habitat. Gene gain and duplication rates behave
359 in general less predictably: numerical differences between loss, gain, and duplica-
360 tion rates on sibling lineages occur in almost all possible sign combinations. The
361 observed fluctuations corroborate the intuition that selection pressures acting on
362 gain and duplication are strong and variable (Wolf *et al.*, 2002). It is plausible that
363 during episodes of massive adaptation, the selective advantages of gene acquisition
364 may outweigh possible negative consequences of an increased genome, and thus
365 drive elevated gene gains, especially if coupled with small population sizes. In our

366 case, unusually large gain rates are inferred on some of the deepest branches (such
367 as the one leading to node E1 on Figure 1 or to the halobacterial ancestor), as well
368 as on the terminal branches leading to *M. acetivorans* (Metac), *H. marismortuimi*
369 (Halma) and *P. aerophilum* (Pyrae).

370 **History of archaeal gene census: streamlining and surges**

371 We inferred a probable history of archaeal gene content using posterior probabili-
372 ties for ancestral family sizes and family size changes, computed from the phylo-
373 genetic profiles in the fitted model. Figure 3 summarizes the results by lineages.
374 (See Supplemental Material for bootstrap confidence intervals: the uncertainty in
375 ancestral family counts is estimated to be within $\pm 19\%$ for all nodes. We note
376 that alternate phylogenies for the Class I methanogens give similar results that fall
377 within those confidence intervals.)

378 [Figure 3 about here.]

379 Our reconstruction suggests a recurrent theme in archaeal evolution: a major
380 physiological or metabolic invention leads to a successful founding population in
381 a new environment, which then further diversifies by genomic streamlining. We
382 can see notably that Figure 3 shows only a few branches where gains prevail over
383 losses (i.e., at least twice as many gains as losses): such is the case for some deep
384 crenarchaeal and euryarchaeal branches, and the terminal lineages for *M. acetivo-*
385 *rans* and *H. marismortuimi*. About half of the remaining terminal lineages and
386 two-thirds of remaining deep lineages are dominated by loss. Moreover, there is
387 only one ancestral node (the crenarchaeal ancestor) in the entire tree for which gain
388 is dominant in both descendant lineages.

389 Why would gene loss be so prevalent? We speculate that the versatility of
390 a large genome in such extant lineages as *M. acetivorans* (Galagan *et al.*, 2002)
391 and *H. marismortuimi* (Baliga *et al.*, 2004) can be upheld for only relatively short
392 time periods. Genetic drift already leads to the diversification of descendant lin-
393 eages, which are frequently isolated, given the disconnectedness of the extreme
394 environments they dwell in (Whitaker *et al.*, 2003; Escobar-Páramo *et al.*, 2005).
395 Specialization and the loss of dispensable functions should be favorable in the de-
396 scendants that are typically under significant energy stress (Valentine, 2007). Ge-
397 nomic streamlining should also be favored by population-size effects due to the
398 isolation (Lynch, 2006), even in the case of slightly deleterious loss of function.

399 After the crenarchaeal split, the main euryarchaeal lineage has been charac-
400 terized by the accumulation of new families, culminating in a large surge on the
401 branch leading to node E1, where many new families appeared. The time interval
402 (judging by sequence divergence in Figure 1) and the extent of gene gain is similar
403 to what is seen with *H. marismortuimi* (Halma) and *M. acetivorans* (Metac). The
404 inference of large gains in the E1 lineage is due to the large number of gene fami-
405 lies shared between multiple descendant lineages, and especially between the two
406 classes of methanogens (Slesarev *et al.*, 2002; Bapteste *et al.*, 2005; Gao and Gupta,
407 2007; Makarova *et al.*, 2007). In fact, this lineage may very well have been where
408 hydrogenotrophic methanogenesis was invented, which then underwent modifica-
409 tions, extensions and degradations in subsequent lineages. It was noted in previous
410 genome-scale comparisons (Bapteste *et al.*, 2005; Gao and Gupta, 2007) that it is
411 likely that euryarchaeal lineages acquired methanogenesis predominantly by verti-
412 cal inheritance, because the associated pathways are fairly complex, and neither the
413 sequences nor the phylogenetic profiles show evidence of substantial amounts of

414 lateral gene transfer. Figure 3 suggests that methanogenesis appeared after the split
415 of Thermococcales in the company of more than 760 genes. Based on extant ex-
416 amples of archaea with such swelled genomes (Galagan *et al.*, 2002; Baliga *et al.*,
417 2004), it is plausible that the corresponding archaeal organisms were extremely
418 versatile.

419 Our inference of ancestral gene content is quite different from previous recon-
420 structions based on parsimony principles (Makarova *et al.*, 2007; Csűrös, 2008): at
421 deep nodes, we postulate larger genomes. Parsimonious reconstructions (Mirkin
422 *et al.*, 2003; Kunin *et al.*, 2005; Csűrös, 2008) aim to minimize the number of im-
423 plied loss and gain events. As a consequence, parsimony inherently underestimates
424 the age of gene families.

425 A major concern in ancestral gene content reconstruction is that “patchy” pro-
426 files arise from a combination of lineage-specific loss events and lateral gene trans-
427 fers (LGT). Frequent lateral gene transfers imply smaller ancestral genome sizes
428 (Dagan and Martin, 2007). Our reconstruction reveals the prevalence of differential
429 loss, but LGT events are far from uncommon. Lineage-specific gains (“Gain col-
430 umn in Figure 3) account to more than 14% of families (“Families in the genome”)
431 at half of all the lineages. A probabilistic framework, such as a phylogenetic
432 birth-and-death model, makes it feasible to take all possible gene family histo-
433 ries into consideration in a mathematically sound way. A case in point is the last
434 archaeal common ancestor (LACA), where only about 1300 families are inferred
435 to have been present with a posterior probability of at least 90%, which is close
436 to a parsimony-based inference of about 1000 families (Makarova *et al.*, 2007).
437 Given the uncertainties of most family histories, the exact genome composition
438 of LACA is hard to estimate, but the fractional probabilities point to a genome

439 with slightly more than 2000 families, which is similar to such extant organisms as
440 *S. sulfolobus*. Such a large genome size implies that LACA's genomic complexity
441 was even greater than previously imagined (Makarova *et al.*, 2007), on a par with
442 modern, moderately-sized archaeal genomes.

443 **Acknowledgments**

444 This work has been supported by a grant from the Natural Sciences and Engineer-
445 ing Research Council of Canada. Part of the study was done while M.Cs. was a
446 sabbatical visitor at the Rényi Institute of Mathematics, supported by a Marie-Curie
447 Transfer-of-Knowledge fellowship. We are grateful to Yuri Wolf for providing data
448 on lineage-specific gene families. We thank Igor Rogozin, Csaba Pál and Balázs
449 Papp for informative discussions.

450 **References**

- 451 Alexeyenko, A., Tamas, I., Liu, G., and Sonnhammer, E. L. L. (2006). Automatic
452 clustering of orthologs and inparalogs shared by multiple genomes. *Bioinform-*
453 *atics*, **22**, e9–e15.
- 454 Baliga, N. S. *et al.* (2004). Genome sequence of *Haloarcula morismurtuimi*: a
455 halophilic archaeon from the Dead Sea. *Genome Research*, **14**, 2221–2234.
- 456 Bapteste, É., Brochier, C., and Boucher, Y. (2005). Higher-level classification of
457 the Archaea: evolution of methanogenesis and methanogens. *Archaea*, **1**, 353–
458 363.
- 459 Boucher, Y., Douady, C. J., Papke, R. T., Walsh, D. A., Boudreau, M. E. R., Nesbo,
460 C. L., Case, R. J., and Doolittle, W. F. (2003). Lateral gene transfer and the
461 origin of prokaryotic groups. *Annual Review of Genetics*, **37**, 283–328.
- 462 Brochier, C., Forterre, P., and Gribaldo, S. (2004). Archaeal phylogeny based
463 on proteins of the transcription and translation machineries: tackling the
464 *Methanopyrus paradox*. *Genome Biology*, **5**, R17.
- 465 Brochier, C., Forterre, P., and Gribaldo, S. (2005). An emerging phylogenetic core
466 of Archaea: phylogenies of transcription and translation machineries converge
467 following addition of new genome sequences. *BMC Evolutionary Biology*, **5**,
468 36.
- 469 Brochier-Armanet, C., Boussau, B., Gribaldo, S., and Forterre, P. (2008).
470 Mesophilic crenarchaeota: proposal for a third archaeal phylum, the Thaumarchaeota.
471 *Nature Reviews Microbiology*, **6**, 245–252.

- 472 Csűrös, M. (2008). Ancestral reconstruction by asymmetric Wagner parsimony
473 over continuous characters and squared parsimony over distributions. *Springer*
474 *Lecture Notes in Bioinformatics*, **5267**, 72–86. Proc. Sixth RECOMB Compar-
475 ative Genomics Satellite Workshop.
- 476 Csűrös, M. and Miklós, I. (2006). A probabilistic model for gene content evolu-
477 tion with duplication, loss, and horizontal transfer. *Springer Lecture Notes in*
478 *Bioinformatics*, **3909**, 206–220. Proc. Tenth Annual International Conference
479 on Research in Computational Molecular Biology (RECOMB).
- 480 Dagan, T. and Martin, W. (2007). Ancestral genome sizes specify the minimum
481 rate of lateral gene transfer during prokaryote evolution. *Proceedings of the*
482 *National Academy of Sciences of the USA*, **104**(3), 870–875.
- 483 Edgar, R. C. (2004). MUSCLE: multiple sequence alignment with high accuracy
484 and high throughput. *Nucleic Acids Research*, **32**(5), 1792–1797.
- 485 Escobar-Páramo, P., Gosh, S., and DiRuggiero, J. (2005). Evidence for genetic
486 drift in the diversification of a geographically isolated population of the hyper-
487 thermophilic archaeon *Pyrococcus*. *Molecular Biology and Evolution*, **22**(11),
488 2297–2303.
- 489 Felsenstein, J. (1981). Evolutionary trees from DNA sequences: A maximum like-
490 lihood approach. *Journal of Molecular Evolution*, **17**, 368–376.
- 491 Felsenstein, J. (1992). Phylogenies from restriction sites, a maximum likelihood
492 approach. *Evolution*, **46**, 159–173.
- 493 Fitz-Gibbon, S. T. and House, C. H. (1999). Whole genome-based phylogenetic

494 analysis of free-living microorganisms. *Nucleic Acids Research*, **27**(21), 4218–
495 4222.

496 Forterre, P., Gribaldo, S., and Brochier-Armanet, C. (2006). Natural history of the
497 archaeal domain. In Garrett and Klenk (2006), chapter 2, pages 17–28.

498 Fricke, W. F. *et al.* (2006). The genome sequence of *Methanosphaera stadtmanae*
499 reveals why this human intestinal archaeon is restricted to methanol and H₂ for
500 methane formation and ATP synthesis. *Journal of Bacteriology*, **188**(2), 642–
501 658.

502 Galagan, J. E., Nusbaum, C., Roy, A., *et al.* (2002). The genome of *M. acetivorans*
503 reveals extensive metabolical and physiological diversity. *Genome Research*,
504 **12**, 532–542.

505 Gao, B. and Gupta, R. S. (2007). Phylogenomic analysis of proteins that are dis-
506 tinctive of Archaea and its main subgroups and the origin of methanogenesis.
507 *BMC Genomics*, **8**, 86.

508 Garrett, R. A. and Klenk, H.-P., editors (2006). *Archaea: Evolution, Physiology,*
509 *and Molecular Biology*. Blackwell Publishing, Malden, Mass.

510 Gogarten, J. P. and Townsend, J. P. (2005). Horizontal gene transfer, genome inno-
511 vation and evolution. *Nature Reviews Microbiology*, **3**, 679–687.

512 Gribaldo, S. and Brochier-Armanet, C. (2006). The origins and evolution of Ar-
513 chaea: a state of the art. *Philosophical Transactions of the Royal Society of*
514 *London, Series B*, **361**, 1007–1022.

- 515 Guindon, S. and Gascuel, O. (2003). A simple, fast, and accurate accurate algo-
516 rithm to estimate large phylogenies by maximum likelihood. *Systematic Biology*,
517 **52**(5), 696–704.
- 518 Hahn, M. W., De Bie, T., Stajich, J. E., Nguyen, C., and Cristianini, N. (2005).
519 Estimating the tempo and mode of gene family evolution from comparative ge-
520 nomic data. *Genome Research*, **15**, 1153–1160.
- 521 Henikoff, S., Greene, E. A., Pietrokovski, S., Bork, P., Atwood, T. K., and Hood, L.
522 (1997). Gene families: the taxonomy of protein paralogs and chimeras. *Science*,
523 **278**, 609–614.
- 524 Hershberg, R., Tang, H., and Petrov, D. A. (2007). Reduced selection leads to
525 accelerated gene loss in *Shigella*. *Genome Biology*, **8**, R164.
- 526 Iwasaki, W. and Takagi, T. (2007). Reconstruction of highly heterogeneous gene-
527 content evolution across the three domains of life. *Bioinformatics*, **23**(13), i230–
528 i239.
- 529 Jordan, M. I. (2004). Graphical models. *Statistical Science*, **19**(1), 140–155.
- 530 Karlin, S. and McGregor, J. (1958). Linear growth, birth, and death processes.
531 *Journal of Mathematics and Mechanics*, **7**(4), 643–662.
- 532 Kendall, D. G. (1949). Stochastic processes and population growth. *Journal of the*
533 *Royal Statistical Society Series B*, **11**(2), 230–282.
- 534 Koonin, E. V. (2005). Orthologs, paralogs, and evolutionary genomics. *Annual*
535 *Review of Genetics*, **39**, 309–338.

- 536 Koonin, E. V. and Wolf, Y. I. (2008). Genomics of bacteria and archaea: the emerg-
537 ing dynamic view of the prokaryotic world. *Nucleic Acids Research*. Advance
538 access published online on October 23, 2008. DOI:10.1093/nar/gkn668.
- 539 Kunin, V., Goldovsky, L., Darzentas, N., and Ouzounis, C. A. (2005). The net
540 of life: reconstructing the microbial phylogenetic network. *Genome Research*,
541 **15**(7), 954–959.
- 542 Lynch, M. (2006). Streamlining and simplification of microbial genome architec-
543 ture. *Annual Review of Microbiology*, **60**, 327–349.
- 544 Makarova, K. and Koonin, E. V. (2005). Evolutionary and functional genomics of
545 the Archaea. *Current Opinion in Microbiology*, **8**, 586–594.
- 546 Makarova, K. S., Sorokin, A. V., Novichkov, P. S., Wolf, Y. I., and Koonin, E. V.
547 (2007). Clusters of orthologous genes for 41 archaeal genomes and implications
548 for evolutionary genomics of archaea. *Biology Direct*, **2**, 33.
- 549 Matte-Tailliez, O., Brochier, C., Forterre, P., and Philippe, H. (2002). Archaeal
550 phylogeny based on ribosomal proteins. *Molecular Biology and Evolution*,
551 **19**(5), 631–639.
- 552 Mira, A., Ochman, H., and Moran, N. A. (2001). Deletional bias and the evolution
553 of bacterial genomes. *Trends in Genetics*, **17**(10), 589–596.
- 554 Mirkin, B. G., Fenner, T. I., Galperin, M. Y., and Koonin, E. V. (2003). Algorithms
555 for computing evolutionary scenarios for genome evolution, the last universal
556 common ancestor and dominance of horizontal gene transfer in the evolution of
557 prokaryotes. *BMC Evolutionary Biology*, **3**, 2.

- 558 Nei, M. and Rooney, A. P. (2005). Concerted and birth-and-death evolution of
559 multigene families. *Annual Review of Genetics*, **39**(1), 121–152.
- 560 Ohta, T. (1972). Population size and rate of evolution. *Journal of Molecular*
561 *Evolution*, **1**, 305–314.
- 562 Pellegrini, M., Marcotte, E. M., Thompson, M. J., Eisenberg, D., and Yeates, T. O.
563 (1999). Assigning protein functions by comparative genome analysis: protein
564 phylogenetic profiles. *Proceedings of the National Academy of Sciences of the*
565 *USA*, **96**(8), 4285–4288.
- 566 Press, W. H., Teukolsky, S. A., Vetterling, W. V., and Flannery, B. P. (1997). *Nu-*
567 *merical Recipes in C: The Art of Scientific Computing*. Cambridge University
568 Press, second edition.
- 569 Rodríguez-Ezpeleta, N., Brinkmann, H., Roure, B., Lartillot, N., Lang, B. F., and
570 Philippe, H. (2007). Detecting and overcoming systematic errors in genome-
571 scale phylogenies. *Systematic Biology*, **56**(3), 389–399.
- 572 Ross, S. M. (1996). *Stochastic Processes*. Wiley & Sons, second edition.
- 573 Slesarev, A. I. *et al.* (2002). The complete genome of hyperthermophile
574 *Methanopyrus kandleri* AV19 and monophyly of archaeal methanogens. *Pro-*
575 *ceedings of the National Academy of Sciences of the USA*, **99**(7), 4644–4649.
- 576 Snel, B., Bork, P., and Huynen, M. A. (1999). Genome phylogeny based on gene
577 content. *Nature Genetics*, **21**(1), 108–110.
- 578 Snel, B., Bork, P., and Huynen, M. A. (2002). Genomes in flux: the evolution of
579 archaeal and proteobacterial gene content. *Genome Research*, **12**(1), 17–25.

- 580 Sonnhammer, E. L. L. and Koonin, E. V. (2002). Orthology, paralogy and proposed
581 classification for paralog subtypes. *Trends in Genetics*, **18**(12), 619–620.
- 582 Spencer, M., Susko, E., and Roger, A. J. (2006). Modelling prokaryote gene con-
583 tent. *Evolutionary Bioinformatics Online*, **2**, 165–186.
- 584 Takács, L. (1962). *Introduction to the Theory of Queues*. Oxford University Press,
585 New York.
- 586 Tatusov, R. L., Koonin, E. V., and Lipman, D. J. (1997). A genomic perspective on
587 protein families. *Science*, **278**, 631–637.
- 588 Tekaiia, F., Lazcano, A., and Dujon, B. (1999). The genomic tree as revealed from
589 whole proteome comparisons. *Genome Research*, **9**(6), 550–557.
- 590 Valentine, D. L. (2007). Adaptations to energy stress dictate the ecology and evo-
591 lution of the Archaea. *Nature Reviews Microbiology*, **5**, 316–323.
- 592 Waters, E. *et al.* (2003). The genome of Nanoarchaeum equitans: insights into
593 early archaeal evolution and derived parasitism. *Proceedings of the National*
594 *Academy of Sciences of the USA*, **100**(22), 12984–12988.
- 595 Whitaker, R. J., Grogan, D. W., and Taylor, J. W. (2003). Geographic barriers
596 isolate endemic populations of hyperthermophilic archaea. *Science*, **301**(5635),
597 976–978.
- 598 Wolf, Y. I., Rogozin, I. B., Grishin, N. V., and Koonin, E. V. (2002). Genome trees
599 and the Tree of Life. *Trends in Genetics*, **18**(9), 472–479.

600 Yang, Z. (1994). Maximum likelihood phylogenetic estimation from DNA se-
601 quences with variable rates over sites: approximate methods. *Journal of Molec-*
602 *ular Evolution*, **39**, 306–314.

603 **List of Figures**

604 1 Consensus evolutionary tree of Archaea in the study. The consen-
605 sus is based on maximum-likelihood trees for concatenated align-
606 ments of ribosomal and unique conserved proteins. Branch lengths
607 are set by maximum likelihood for the ribosomal proteins. Rec-
608 ognized archaeal orders are highlighted. The boxed triples on the
609 left show the percentage of bootstrap samples supporting the par-
610 ticular edges in three data sets (from 500 replicates for each set): r-
611 proteins, uc-proteins, and uc-proteins without *C. symbiosum* (Censy)
612 and *N. equitans* (Naneq). All other edges have > 97% bootstrap
613 support in all data sets. Numbers next to the terminal taxa denote
614 genome size in million base pairs. 31

615 2 Branch-specific loss rates $\hat{\mu}_e \hat{t}_e$ compared to expected numbers of
616 substitutions (or *edge length*) for each branch *e*. Pairs of sibling
617 terminal taxa are connected by lines. 32

618 3 A digest of gene content evolution in Archaea. The bar graphs
619 plot posterior means for number of families. The chart **on the left**
620 shows the number of families with at least one homolog; the fatter
621 part of the bar is proportional to the number of multi-gene families.
622 The chart **in the middle** plots the families acquired and lost on the
623 branch leading to the indicated node. The net change is highlighted
624 by the solid part of the bars. The chart **on the right** shows how
625 many families underwent a contraction from multi-gene to single-
626 gene composition, or expanded from a single homolog to multiple
627 paralogs. For instance, the common ancestor of Methanococcales
628 is inferred to have had 1723 gene families, out of which 156 were
629 gained after the split with Methanobacteriales. During the same
630 time, 586 families present at the common ancestor M1 were lost,
631 and the solid bar indicates the net loss of 430 (=586-156) families.
632 Among multi-member families retained from M1, 68 contracted to
633 a single homolog, and 13 single-member families expanded. Note
634 that scaling is the same on the left-hand side and in the middle, but
635 different on the right-hand side. 33

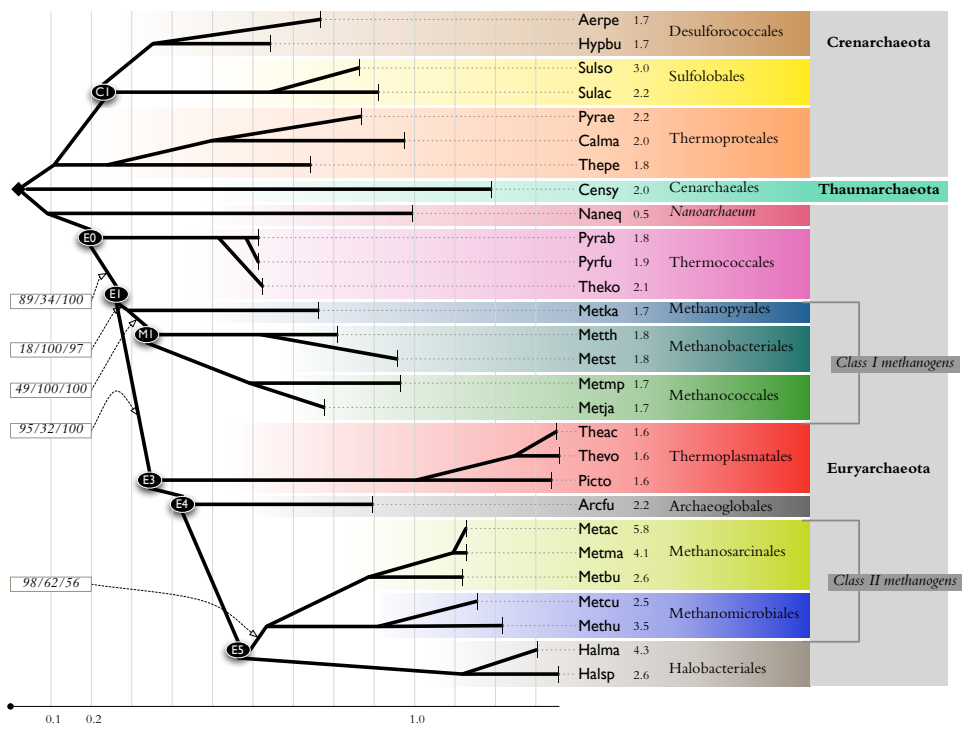


Figure 1

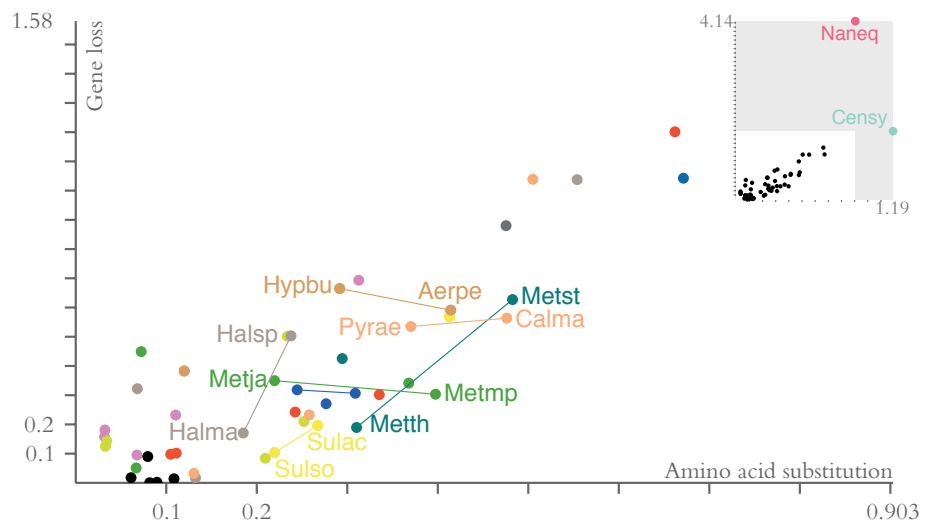


Figure 2

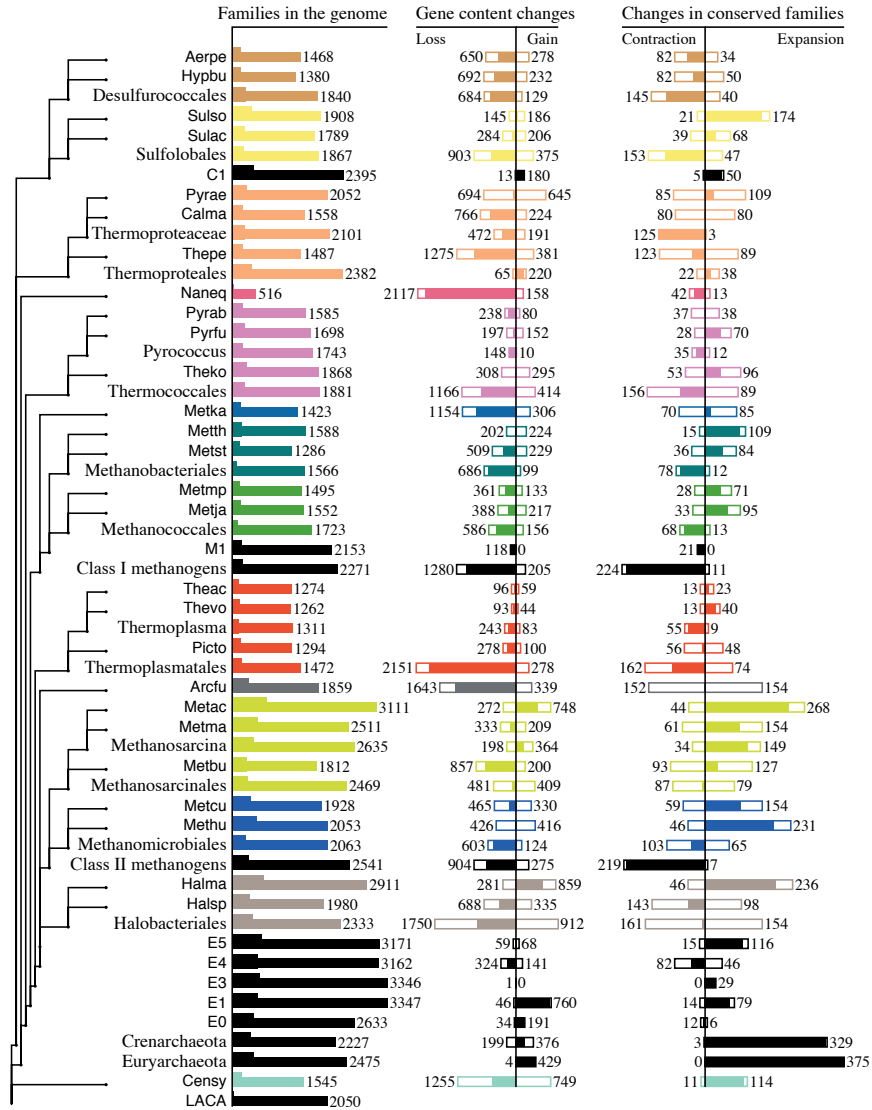


Figure 3